# Limited sensitivity analysis of regional climate change probabilities for the 21st century

Suraje Dessai,[1] Xianfu Lu,[1] and Mike Hulme[1]
School of Environmental Sciences, University of East Anglia, Norwich, UK

Received 27 February 2005; revised 30 June 2005; accepted 25 July 2005; published 8 October 2005.

[1] Quantifying uncertainty in regional climate change projections is important for a range of reasons. We examine the sensitivity of regional climate change probabilities to various uncertainties. We use a simple probabilistic energy balance model that samples uncertainty in greenhouse gas emissions, the climate sensitivity, the carbon cycle, ocean mixing, and aerosol forcing. We then propagate global mean temperature probabilities to General Circulation Models (GCMs) through the pattern-scaling technique. In order to combine the resulting probabilities we devised regional skill scores for each GCM, season (DJF, JJA), and climate variable (surface temperature, and precipitation) in 22 world regions, based on model performance and model convergence. A range of sensitivity experiments are carried out with different skill score schemes, climate sensitivities, and emissions scenarios. It was shown that whether skill scores as applied in this paper were used or not, makes little difference to regional climate change probabilities. However, both these approaches provide more information than simply using the multi-model ensemble average. For temperature change probabilities, emissions scenarios uncertainty tends to dominate the 95th percentile whereas climate sensitivity uncertainty plays a more important role at the 5th percentile. The sensitivity of precipitation change probabilities to the tested uncertainties are region specific, but some conclusions can be drawn. At the 95th percentile, the uncertainty that tends to dominate is emissions scenarios, closely followed by GCM weighting scheme and the climate sensitivity. At the 5th percentile, GCM weighting scheme uncertainty tends to dominate for JJA, but for DJF all uncertainties have similar proportionate influence.

**Citation:** Dessai, S., X. Lu, and M. Hulme (2005), Limited sensitivity analysis of regional climate change probabilities for the 21st century, *J. Geophys. Res.*, *110*, D19108, doi:10.1029/2005JD005919.

## 1. Introduction

[2] The IPCC Third Assessment Report concluded there was evidence that most of the warming observed over the last 50 years is attributable to human activities [*Houghton et al.*, 2001]. With the expected build-up of greenhouse gases in the atmosphere, it is anticipated that the climate will continue to change throughout the 21st century. The nature of future regional changes in climate is much less certain than global changes because of the compounding of uncertainties. Several global studies have attempted to quantify uncertainties explicitly such as the likelihood of sea level rise [*Patwardhan and Small*, 1992; *Titus and Narayanan*, 1996] and global mean temperature change [*Dessai and Hulme*, 2001; *Morgan and Keith*, 1995; *Stott and Kettleborough*, 2002; *Visser et al.*, 2000; *Webster et al.*, 2003; *Wigley and Raper*, 2001]. Most of these studies included some subjective assessment (based on expert judgement) of certain key uncertain parameters (e.g., climate sensitivity). Increasingly, quasi-objectively determined distributions of these parameters have been estimated by constraining climate models with recent observed data [*Andronova and Schlesinger*, 2001; *Forest et al.*, 2002; *Gregory et al.*, 2002; *Knutti et al.*, 2002; *Murphy et al.*, 2004; *Tol and de Vos*, 1998]. With increasing computational power, these techniques are expected to generate a climate change forecast based on 'super-ensembles' [*Allen*, 1999; *Stainforth et al.*, 2002, 2005].

[3] Inadequate quantification of uncertainties in regional climate projections has been a major shortfall for impact and adaptation assessments of climate change [*Carter et al.*, 2001]. These uncertainties arise from a number of sources: (1) propagation of 'upstream' uncertainties associated with future greenhouse gas emissions and their atmospheric concentration, and global climate sensitivity; (2) different General Circulation Models (GCMs) yield different regional climate responses, even when they are perturbed with identical forcing; (3) the multitude of techniques available to simulate sub-GCM scale regional distributions of climate. In general, these uncertainties have been estimated by

[1]Also at Tyndall Centre for Climate Change Research, UK.


0148-0227/05/2005JD005919$09.00

comparing different GCMs and different emissions scenarios in several regions around the world [*Giorgi and Francisco*, 2000a; *Giorgi and Mearns*, 2002; *Hulme and Brown*, 1998; *Kittel et al.*, 1998; *Ruosteenoja et al.*, 2003]. Some recent studies have considered GCM outputs (the so-called 'ensembles of opportunity') as a multi-model ensemble to derive frequency distributions of future regional climate [*Benestad*, 2004; *Ekström et al.*, 2005; *Jones*, 2000a; *New and Hulme*, 2000; *Palmer and Räisänen*, 2002; *Räisänen and Alexandersson*, 2003; *Räisänen and Palmer*, 2001]. These approaches fit better with the identification of appropriate management responses regarding adaptation to climate change [*Jones*, 2000b], now increasingly recognised as a priority response to our changing climate [*Adger et al.*, 2005; *Parry et al.*, 1998].

[4] More sophisticated approaches for generating regional probabilities are now emerging. *Giorgi and Mearns* [2003] extended their Reliability Ensemble Averaging method [see *Giorgi and Mearns*, 2002] to calculate regional probabilities of climate change. *Tebaldi et al.* [2004, 2005] developed a full Bayesian probabilistic model of regional climate change. The European ENSEMBLES project is also developing further methods of constructing regional climate change probabilities (http://www.ensembles-eu.org/).

[5] In this paper, we develop a simple probabilistic framework for regional climate scenario construction and test the sensitivity of regional climate change probabilities to key parameters. The framework is simple because it makes use of global temperature change projections from a simple energy-balance climate model [*Wigley and Raper*, 2001] (hereinafter referred to as WR01) to represent uncertainties in emissions scenarios, climate sensitivity and other model parameters. Recent estimates of the probability density function (PDF) of climate sensitivity [e.g., *Andronova and Schlesinger*, 2001; *Forest et al.*, 2002; *Knutti et al.*, 2002; *Tol and de Vos*, 1998] can thus be used to represent uncertainty in physical processes and feedbacks. Uncertainty in future world development and greenhouse gas emissions is represented by scenario analysis using the IPCC Special Report on Emissions Scenarios (SRES) [*Nakicenovic et al.*, 2000]. The rationale for this is to combine state-of-the-art research within a framework that explicitly represents uncertainty throughout a climate assessment. The framework is probabilistic because the simple climate model outputs global mean temperature change PDFs that we combine with publicly available GCM simulations using the "pattern-scaling" technique originally developed by *Santer et al.* [1990]. We evaluate the GCM simulations at a regional scale using the criteria of model performance and model convergence. We use these criteria to calculate regional skill scores for each GCM, season and variable which allows the combinations of different GCM PDFs into a single PDF, thus representing uncertainty in regional climate change from GCM experiments. We perform a range of analyses to test the relative sensitivity of probabilistic regional climate change to different sources of uncertainty.

[6] The main objectives of this paper therefore are twofold: first, to illustrate a probabilistic framework that quantifies a range of uncertainties in constructing regional projections of climate change; second, to test the relative sensitivity of regional probabilities of climate change to different sources of uncertainty.

## 2. Methodology

### 2.1. Probabilities of Global Temperature Change

[7] Probabilistic estimates of global mean temperature change were calculated using the *Wigley and Raper* [2001] model (probabilistic version of MAGICC). MAGICC is a coupled gas-cycle/energy-balance, upwelling-diffusion climate model. (A user-friendly version of the model may be downloaded from http://www.cgd.ucar.edu/.) The probabilistic version of MAGICC allows the representation of uncertainties from greenhouse gas emissions, climate sensitivity, carbon cycle, ocean mixing and aerosol forcing as input PDFs to drive the model. MAGICC uses exhaustive fractile sampling, which "considers all possible combinations of results for the division of the input distribution into prespecified fractiles" [*Wigley and Raper*, 2001]. For example, for climate sensitivity the model uses 25 fractiles and for carbon cycle, ocean mixing and aerosol forcing the model uses quintiles. Therefore, for each greenhouse gas scenario the model outputs 3125 simulations ($25 \times 5 \times 5 \times 5$).

[8] Uncertainties associated with greenhouse gas emissions were represented through the use of scenarios (i.e., plausible futures, not predictions or forecasts), because this type of uncertainty is difficult to quantify, whereas other parameter uncertainties were quantified using expert judgement based PDFs from WR01 and other PDFs available in the literature. We used all 35 complete scenarios of the IPCC's Special Report on Emissions Scenarios, but each scenario was grouped into their respective scenario family (SRES A1, A2, B1, B2). Therefore SRES A1 was represented by 15 scenarios, SRES A2 by six scenarios, SRES B1 by eight scenarios and SRES B2 by six scenarios.

### 2.2. GCM Regional Skill Scores

[9] Any attempt to assign probabilities to regional climate change projections should pass through the phase of model evaluation. Model evaluation has been a standard element in the IPCC assessments [e.g., *Gates et al.*, 1996; *McAvaney et al.*, 2001], model intercomparison projects [e.g., *Gates et al.*, 1999; *Lambert and Boer*, 2001] and various national assessments [e.g., *MacCracken et al.*, 2001; *Miranda et al.*, 2002]. The methodology applied here is simultaneously simpler and more complex than past efforts. It is simpler because out of the numerous output variables of GCMs we only focus our attention on two: surface air temperature and precipitation (see *Murphy et al.* [2004], who use a Climate Prediction Index with 32 components). We do not analyse the individual processes and model components [cf. *Stocker et al.*, 2001]. It is more complex because we go beyond the descriptive statistics of GCMs (e.g., global means, regional averages or geographical distributions), into the arena of defining model skill and translating it into regional climate change probabilities.

[10] Traditionally, model evaluation can be divided into two major efforts. First, how well can the model simulate current climate? Second, how consistently do the different models respond to the same forcing (e.g., doubling $CO_2$ concentrations)? *Wigley* [1999] performed such a model

evaluation for an earlier set of GCM experments, while *Giorgi and Mearns* [2002] used the same data set analysed here. The latter authors called these two criteria "model performance" and "model convergence", which we shall also use. In model performance, GCM baseline period results are compared to observations whereas in model convergence GCM forced experiments are compared with the multi-model ensemble average. Our evaluation has relied on a modified version of the least complicated skill score we could find in the literature based on *Taylor* [2001] [see also *Murphy*, 1988; *Watterson*, 1996]. For two data series $X_1$ and $X_0$, which are measurements for variable $x$, the ratio of the absolute value of the average of series $X_0$ to the mean square-root error of $X_1$ and $X_0$ is used to estimate the similarity of $X_1$ to $X_0$ (see equation (1) below).

$$S = \frac{|\bar{x}_0|}{\left[\frac{1}{N}\sum_{i=1}^{N}(x_{i1} - x_{i0})^2\right]^{1/2}} \tag{1}$$

where

$N$: number of data points (grid cells);
$x_{i1}$: the $i$th data point of series $X_1$ for variable $x$;
$x_{i0}$: the $i$th data point of series $X_0$ for variable $x$;
$\bar{x}_0$: average of $X_0$ for variable $x$.

Applying this skill score, we estimate model performance using equation (2)

$$S_{performance} = \frac{|\bar{x}_{obs}|}{\left[\frac{1}{N}\sum_{i=1}^{N}(x_{i\,\mathrm{mod}} - x_{iobs})^2\right]^{1/2}} \tag{2}$$

where

$S_{performance}$: model performance skill score;
$N$: number of data points (grid cells);
$x_{i\ \mathrm{mod}}$: the $i$th data point of model simulation for variable $x$;
$x_{iobs}$: the $i$th data point of observations for variable $x$;
$\bar{x}_0$: average of observations for variable $x$.

This skill score includes overall model bias, spatial variance, and pattern correlation [cf. *Taylor*, 2001, pp. 7183–7184], hence represents an integrated index for measuring model performance.

[11] Similarly, convergence skill score can be calculated using equation (3):

$$S_{j,convergence} = \frac{|\bar{x}_{ens}|}{\left[\frac{1}{N}\sum_{i=1}^{N}(x_{ij} - x_{iens})^2\right]^{1/2}} \tag{3}$$

where

$S_{j,convergence}$: convergence skill score of model $j$;
$N$: number of data points (grid cells);
$x_{ij}$: the $i$th data point of model $j$ simulation for variable $x$;
$x_{iens}$: the $i$th data point of the ensemble average for variable $x$;
$\bar{x}_{ens}$: regional multi-model ensemble average for variable $x$.

The skill score is applied separately to each GCM (see Table 1), each season (DJF and JJA), each variable (surface temperature and precipitation) and each region (see Table 2). The combined regional skill score comprises the skill scores of model performance and model convergence. It is calculated by

$$S = \left(\sqrt{S_{performance}} \times \sqrt{S_{convergence}}\right)^4 \tag{4}$$

Two sets of data are used to derive the skill scores described above:

[12] 1. Observational data set: The Climatic Research Unit (CRU) 0.5 by 0.5 degree 1961 ~ 1990 average monthly temperature and precipitation climatologies (downloadable at http://ipcc-ddc.cru.uea.ac.uk/obs/get_30yr_means.html) [*New et al.*, 1999] are used to calculate the performance skill score. To be compatible with the GCM simulations (see below), baseline temperature and precipitation climatologies are aggregated onto a 2.5 by 2.5 degree grid, by simple averaging the values of 0.5 degree grid cells falling within the corresponding 2.5 degree grid box. Monthly fields are also averaged to produce seasonal mean climatologies.

[13] 2. GCM simulations: Seasonal temperature and precipitation fields from simulations performed with nine GCMs and forced by the SRES A2 emissions scenarios (see Table 1) are analyzed in this paper. Simulations for the periods of 1961 ~ 90 and 2071 ~ 2100 are used to represent baseline climatologies and changed climatic conditions, respectively. These GCM simulated climate fields are regridded from their native grids to a 2.5 by 2.5 degree grid.

### 2.3. Probabilities of Regional Climate Change

[14] We combined the PDFs of global mean temperature change from the simple climate model with the GCM results using the pattern scaling technique. Original GCM patterns are normalised by the global average temperature change as simulated by the same GCM forced by the same emissions scenario and for the same time period. Then normalised GCM response patterns of regional climate change are scaled by global average temperature change (from simple climate models) to derive regional climate change scenarios. Since global average temperature changes can be rapidly simulated by simple climate models for a range of emissions scenarios, climate sensitivities, and other model parameterizations, pattern scaling enables the exploration of sensitivity of regional climate responses to key uncertainty sources, such as structural differences in climate models, difference in emissions trajectories, and climate sensitivity uncertainty. Here we use global temperature change simulations from the probabilistic MAGICC version as scalars.

[15] For generating regional climate change scenarios under a certain emissions scenario, Monte Carlo selection of GCM is made according to the skill score (i.e., the higher the skill score of a GCM the more times that GCM gets selected according to a linear relationship between skill and weighting) to obtain regional normalised GCM simulation, which is then scaled by one of the 3125 MAGICC simulated global temperature change projections under the same emissions scenario (this is named weighting scheme A). Consequently, there are in total 3125 × N (N – number of

**Table 1.** GCMs With Which Experiments Forced by SRES A2 Emissions Scenarios Were Performed and Global Temperature and Precipitation Patterns Derived[a]

| GCM | Atmospheric Resolution | Ocean Resolution | Center | Global Temperature Change by the 2080s[b] | Reference |
|---|---|---|---|---|---|
| CSM 1.3 | 2.8° × 2.8° L18 | 2.0° × 2.4° L45 | NCAR | 2.7 | [*Boville et al.*, 2001] |
| CGCM2 | 3.8° × 3.8° L10 | 1.8° × 1.8° L29 | CCCma | 4.3 | [*Flato and Boer*, 2001] |
| CSIRO Mk2 | 3.2° × 5.6° L9 | 3.2° × 5.6° L21 | CSIRO | 4.1 | [*Gordon and O'Farrell*, 1997] |
| ECHAM4/OPYC3 | 2.8° × 2.8° L19 | 2.8° × 2.8° L11 | DKRZ | 3.6 | [*Roeckner et al.*, 1996] |
| GFDL_R15_b | 4.5° × 7.5° L9 | 4.5° × 3.7° L12 | GFDL | 3.5 | [*Dixon and Lanzante*, 1999] |
| DOE PCM | 2.8° × 2.8° L18 | 0.67° × 0.67° L32 | NCAR | 2.6 | [*Washington et al.*, 2000] |
| CCSR/NIES2 | 5.6° × 5.6° L20 | 2.8° × 3.8° L17 | CCSR/NIES | 5.3 | [*Nozawa et al.*, 2000] |
| HadCM3 | 2.5° × 3.75° L19 | 1.25° × 1.25° L20 | UKMO | 3.8 | [*Gordon et al.*, 2000] |
| MRI2 | 2.8° × 2.8° L30 | 2.0° × 2.5° L23 | MRI | 1.6 | [*Yukimoto et al.*, 2000] |

[a]Adopted from *McAvaney et al.* [2001, Table 8.1].
[b]Model simulated, SRES A2-forced, global annual average temperature rise (°C) of the 30-year period centered on the 2080s with respect to that of the 1961 ∼ 1990 period.

emissions scenarios under each SRES scenario families) regional scenarios for each region, each variable and each season. They form the basis for the construction of regional climate change cumulative distribution functions (CDFs). We also present results without using skill scores (NS, no skill), where each GCM has the same weight, and using the GCM ensemble mean (EN) without any weighting, both in conjunction with global temperature change probabilities. In addition, for weighting scheme A, we show results as probabilities of exceeding thresholds.

### 2.4. Sensitivity of Regional Climate Change Probabilities

[16] In order to test the sensitivity of our results we performed four sets of experiments for all regions for each season (DJF, JJA) and each climate variable (surface temperature and precipitation). The first experiment compares results using the combined skill score for performance and convergence (weighting scheme A), no skill score (NS) and the GCM ensemble average (EN), for 2100 under SRES A2 using the WR01 climate sensitivity PDF. The second experiment uses weighting scheme A and explores the differences between SRES scenario families (SRES A1, A2, B1 and B2) for 2100 using the WR01 climate sensitivity PDF. The third experiment uses scheme A, under SRES A2, using the WR01 climate sensitivity PDF, but changes the time horizon (2020, 2050, 2100). The final experiment uses different probability density functions for climate sensitivity other than the one used in WR01, namely the uniform *Forest et al.* [2002] and *Andronova and Schlesinger* [2001] for 2100 using weighting scheme A. In order to quantify the sensitivity of the resulting probabilities we estimated the magnitude of the uncertainty range for different weighting schemes, climate sensitivities and SRES scenario families. This uncertainty range was calculated by subtracting the maximum value of the CDF by the minimum value at the 5th, 50th, and 95th percentile for each region, season, and climate variable.

## 3. Results

### 3.1. Sensitivity of Global Temperature Change to Emissions Scenarios and Climate Sensitivity Uncertainties

[17] Figure 1 shows the probability of global mean temperature change for each of the SRES scenario families

**Table 2.** List of Regions Used in This Study[a]

| | Name | Acronym | Latitude ° | Longitude ° |
|---|---|---|---|---|
| 1 | Northern Australia | NAU | 28S ∼ 11S | 110E ∼ 155E |
| 2 | Amazon Basin | AMZ | 20S ∼ 12N | 82W ∼ 34W |
| 3 | Southern South America | SSA | 56S ∼ 20S | 76W ∼ 40W |
| 4 | Central America | CAM | 10N ∼ 30N | 116W ∼ 83W |
| 5 | Western North America | WNA | 30N ∼ 60N | 130W ∼ 103W |
| 6 | Central North America | CNA | 30N ∼ 50N | 103W ∼ 85W |
| 7 | Eastern North America | ENA | 25N ∼ 50N | 85W ∼ 60W |
| 8 | Alaska | ALA | 60N ∼ 72N | 170W ∼ 103W |
| 9 | Greenland | GRL | 50N ∼ 85N | 103W ∼ 10W |
| 10 | Mediterranean Basin | MED | 30N ∼ 48N | 10W ∼ 40E |
| 11 | Northern Europe | NEU | 48N ∼ 75N | 10W ∼ 40E |
| 12 | Western Africa | WAF | 12S ∼ 18N | 20W ∼ 22E |
| 13 | Eastern Africa | EAF | 12S ∼ 18N | 22E ∼ 52E |
| 14 | Southern Africa | SAF | 35S ∼ 12S | 10W ∼ 52E |
| 15 | Sahara | SAH | 18N ∼ 30N | 20W ∼ 65E |
| 16 | Southeast Asia | SEA | 11S ∼ 20N | 95E ∼ 155E |
| 17 | East Asia | EAS | 20N ∼ 50N | 100E ∼ 145E |
| 18 | South Asia | SAS | 5N ∼ 30N | 65E ∼ 100E |
| 19 | Central Asia | CAS | 30N ∼ 50N | 40E ∼ 75E |
| 20 | Tibet | TIB | 30N ∼ 50N | 75E ∼ 100E |
| 21 | North Asia | NAS | 50N ∼ 70N | 40E ∼ 180E |
| 22 | Southern Australia | SAU | 45S ∼ 28S | 110E ∼ 155E |

[a]From *Giorgi and Francisco* [2000b].

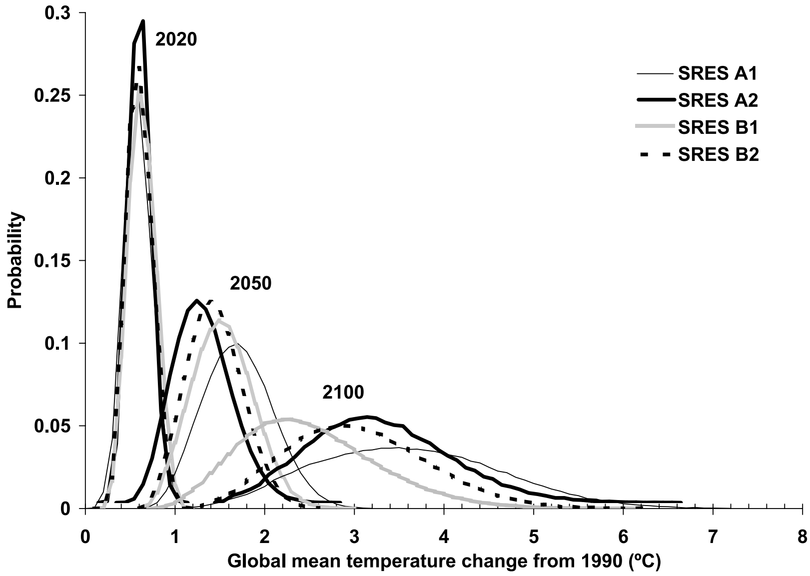


**Figure 1.** Probability of global mean temperature change from 1990 for 2020, 2050, and 2100 under the four SRES scenarios families (SRES A1, A2, B1, and B2). Bins of 0.1°C.

at different time horizons when an expert log-normal distribution for climate sensitivity (used in WR01) is applied, with the same PDFs as in the original paper for the other parameters. SRES A1 has a flatter distribution than the other three scenario families because it includes scenarios with different assumptions about technology and resource dynamics, which produce substantially different greenhouse gas emissions by the end of the century. Greenhouse gas emission uncertainty is rather small in 2020, in terms of global mean temperature change, but expands over time. It is curious to note that SRES A2 has the lowest global temperature change compared to the other scenario families in 2050 even though it has high $CO_2$ emissions. This occurs because this scenario family has the highest $SO_2$ emissions, which has a considerable impact on global temperature change. By 2100 $SO_2$ emissions have dropped enough to make greenhouse gas emissions the main driver of global temperature change.

[18] Climate sensitivity is a particularly uncertain parameter. Figure 2 presents the probability of global mean temperature change in 2100 under the SRES A2 scenario family using six PDFs of climate sensitivity from recent studies. Under this range of climate sensitivity distributions, there is some chance that global mean temperature change is outside the IPCC TAR range of 1.4–5.8°C, particularly at the high end of the range.

### 3.2. GCM Regional Skill Scores

[19] Figure 3 shows the skill scores for each GCM for each region of Table 2 for model performance and model convergence (for each season and climate variable). For performance, skill scores are usually higher for temperature

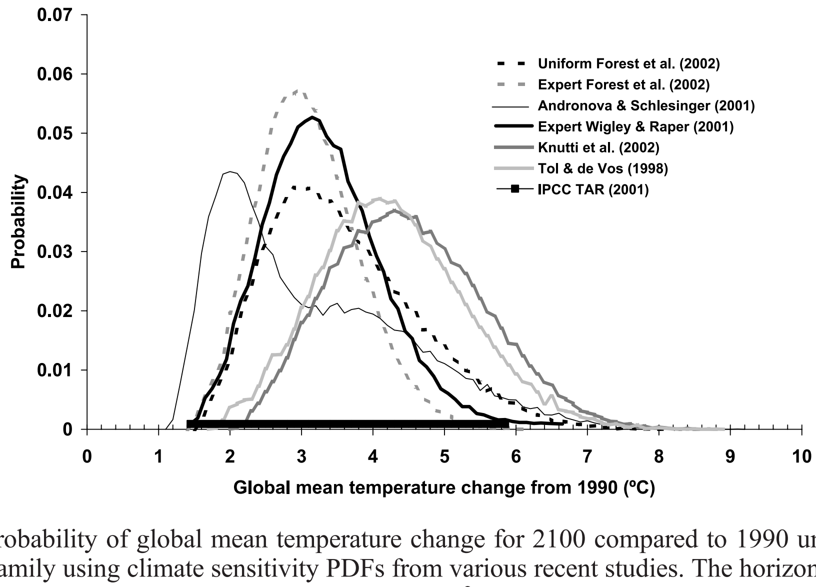


**Figure 2.** Probability of global mean temperature change for 2100 compared to 1990 under the SRES A2 scenario family using climate sensitivity PDFs from various recent studies. The horizontal thick black line represents the IPCC TAR (2001) range. Bins of 0.1°C.

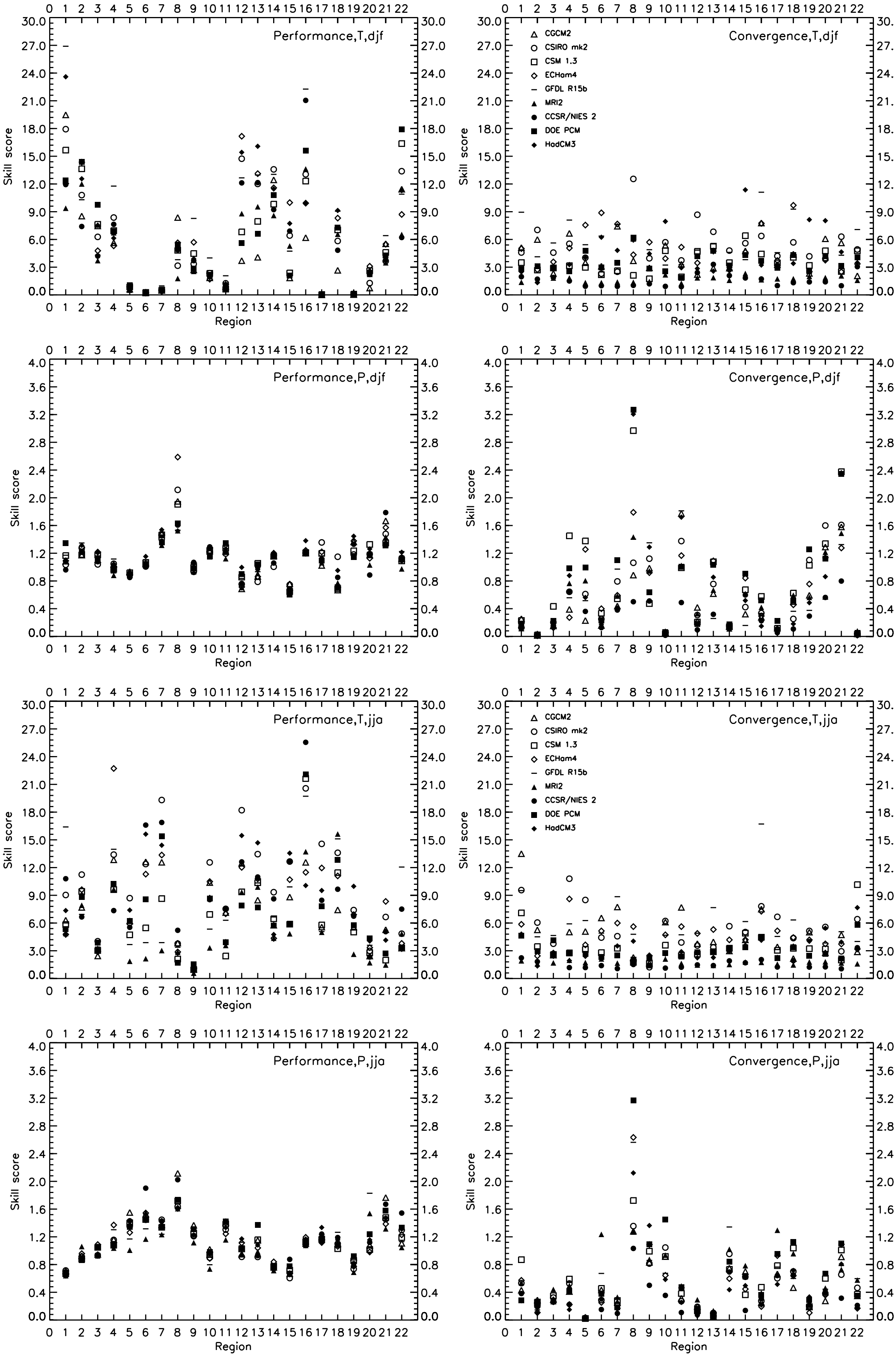


**Figure 3.** Regional skill scores for each GCM, for model performance and model convergence for DJF and JJA, temperature (T) and precipitation (P) for each of the 22 regions.

**Table 3.** Mean Skill Score (for Performance and Convergence) for Each Global Climate Model (Averaged Over the 22 Regions) for Each Season and Climate Variable

| | | Temperature | | Precipitation | |
|---|---|---|---|---|---|
| | | Performance | Convergence | Performance | Convergence |
| DJF | CGCM2 | 4.68 | 4.26 | 1.14 | 0.51 |
| | CSIRO mk2 | 6.16 | 5.36 | 1.14 | 0.59 |
| | CSM 1.3 | 5.71 | 3.53 | 1.14 | 0.78 |
| | ECHam4 | 6.33 | 4.93 | 1.18 | 0.59 |
| | GFDL R15b | 7.49 | 5.67 | 1.12 | 0.50 |
| | MRI2 | 4.76 | 1.69 | 1.06 | 0.56 |
| | CCSR/NIES 2 | 5.56 | 1.57 | 1.11 | 0.30 |
| | DOE PCM | 5.82 | 3.52 | 1.11 | 0.77 |
| | HadCM3 | 6.72 | 4.56 | 1.18 | 0.65 |
| JJA | CGCM2 | 7.04 | 4.86 | 1.18 | 0.47 |
| | CSIRO mk2 | 9.99 | 5.34 | 1.09 | 0.49 |
| | CSM 1.3 | 6.31 | 3.53 | 1.12 | 0.57 |
| | ECHam4 | 8.15 | 4.69 | 1.12 | 0.51 |
| | GFDL R15b | 7.51 | 5.81 | 1.16 | 0.56 |
| | MRI2 | 5.00 | 1.70 | 1.04 | 0.63 |
| | CCSR/NIES 2 | 8.92 | 1.61 | 1.19 | 0.32 |
| | DOE PCM | 7.12 | 3.04 | 1.17 | 0.66 |
| | HadCM3 | 8.22 | 3.30 | 1.15 | 0.45 |

than precipitation. Convergence skill scores vary widely showing the discrepancy between individual GCM simulations and the ensemble mean. We also present the average skill score across the regions for performance and convergence for each GCM (Table 3).

[20] As shown in Figure 3, regional skill scores of GCMs do not show consistent trends across regions, seasons, or variables. That is to say, a GCM with high skill score for one variable, in one season, for one region does not imply that it has high skill score for another variable, in a different season, or for another region.

### 3.3. Sensitivity of Regional Climate Change Probabilities

[21] The number of results using different combinations of the components within the framework proposed in this paper is potentially very large. Therefore, we only show results for the sensitivity tests.

[22] The first set of results (Figures 4 and 5) illustrates the sensitivity of regional climate change probabilities to different GCM weighting schemes. The schemes have little impact on temperature in general, with the exception of DJF in Figure 4, whereas precipitation is more sensitive. But the sensitivity is region specific, as shown in Figure 4 for temperature in Northern Europe. Most other regions are insensitive to weighting schemes as in the right panels (JJA) of Figures 4 and 5. Overall, the ensemble mean scheme provides the narrowest distribution and is thus the most distinguishable scheme. This is not surprising since this scheme only uses one value whereas the other schemes use nine GCM results (either weighted or not). In most regions the combined skill score (A) scheme and the no skill score scheme (NS) are very close to each other. We have three explanations for this: (1) the skill scores applied here are not a good constraint on probabilities of regional climate change; (2) the span of GCM simulations used in this study is not sufficiently large to make the PDFs distinguishable; (3) there is a certain degree of similarity between GCMs and their response to forcings. It is worth noting that the ensemble mean approach underestimates precipitation change considerably when compared to the other approaches (this is particularly clear in Figure 5 for West Africa).

[23] Figures 6, 7, and 8 present the sensitivity of regional climate change probabilities to greenhouse gas emission uncertainty, for scheme A in 2100 using the WR01 climate sensitivity for Alaska, Central North America, and Amazon Basin, respectively. Different SRES scenario families can have a substantial impact on temperature change. The difference between scenarios is biggest at higher latitudes where the largest warming occurs. There is a similar, but of smaller magnitude, effect for precipitation; SRES B1 produces the smallest precipitation change whereas SRES A1 produces the largest.

[24] Time horizon plays an important role in the construction of regional climate change probabilities, perhaps the most important one, with small changes in the near future and large changes predicted for the end of the century. Figure 9 shows results under weighting scheme A for SRES A2 with WR01 climate sensitivity PDF under different time lines (2020, 2050, and 2100) for the Mediterranean region.

[25] Similarly, changing the climate sensitivity from the expert WR01 changes the shape of the distributions, in particular the tails. Figure 10 shows the example of East Africa.

[26] By presenting the range (maximum value minuses minimum value) of various percentile regional temperature and precipitation changes under different types of uncertainties, Table 4 shows the sensitivity of regional climate change probabilities (for DJF) to different sources of uncertainties. Thus, the higher the number the more sensitive the region is to that particular uncertainty. For temperature, the uncertainty introduced by GCM weighting scheme on regional probabilities of temperature change are very small (rarely above 1°C). At the lower end of the distribution (95%), SRES uncertainty tends to dominate whereas at the upper end (5%) climate sensitivity uncertainty plays a slightly more important role. For precipitation, the results vary by region. At the lower end of the precipitation distribution, the uncertainty that tends to dominate is SRES, closely followed by GCMs and climate sensitivity. At the upper end, GCMs tend to dominate for JJA, but for DJF all uncertainties are relatively similar.

### 3.4. Probability of Regional Climate Change Exceeding Thresholds

[27] Table 5 presents the probabilities of regional temperature and precipitation change exceeding certain thresholds under SRES A2 scenarios, with WR01 climate sensitivity PDF, and GCM weighting scheme A for 2100 for the same group of regions as in *Giorgi and Mearns* [2003]. For temperature, Northern Europe (NEU) has the highest probabilities of experiencing above 4 and 6°C warming in DJF; while Central North America (CNA) stands the largest chance of warming up by more than 4 and 6°C in JJA. West Africa (WAF) has the highest probability of experiencing more than 10 percent reduction in DJF rainfall while Northern Europe (NEU) is most likely to experience more than 10 percent increase in DJF precipitation. For JJA precipitation, Southern Africa (SAF) is most likely to experience more than 10 percent reduction while Southern Asia (SAS) stands the highest chance of experiencing more than a 10 percent increase.

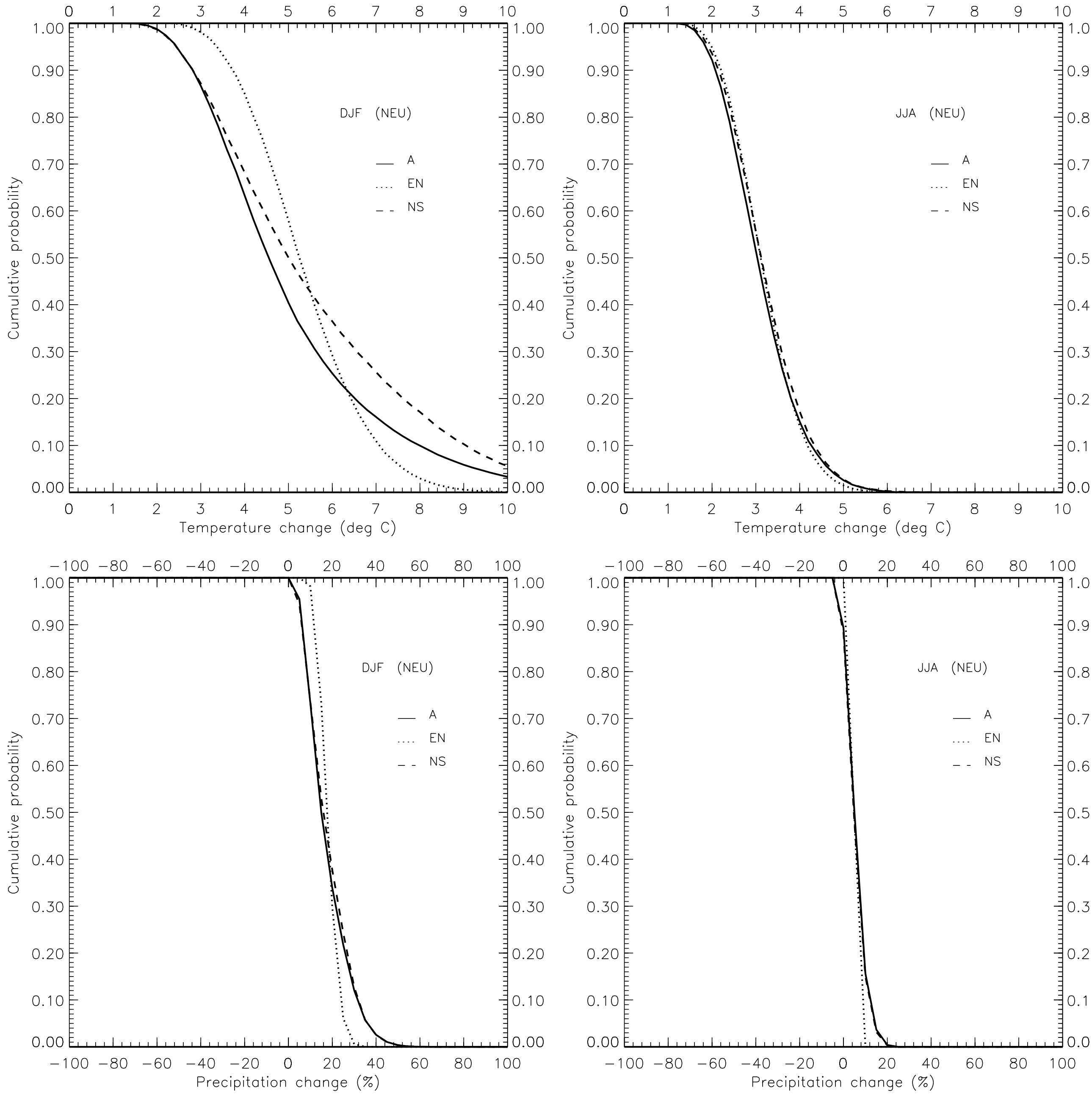


**Figure 4.** Regional cumulative probabilities of temperature and precipitation change for each season (DJF, JJA) for Northern Europe under three different weighting schemes: using the combined skill score (A), using the ensemble mean (EN), and using no skill scores (NS). These probabilities are calculated for 2100 under the SRES A2 scenario family using the WR01 climate sensitivity PDF.

[28] These probabilities of climate change exceeding thresholds are compared with those in *Giorgi and Mearns* [2003] (see values in parentheses in Table 5). With a few exceptions, these two sets of values are generally comparable. Differences between them would result from: different definitions of skill scores, different underlying emissions scenarios, and size of samples for estimating the probabilities. *Giorgi and Mearns* [2003] used both SRES A2 and B2 simulations, while estimates from this paper are based on SRES A2 scenarios only. *Giorgi and Mearns* [2003] used both A2 and B2 simulations performed with nine GCMs (hence 18 samples), while this paper contains a sample of 18750 (3125 global temperature change samples and six SRES A2 scenario family members.

## 4. Discussion and Conclusions

[29] In this paper, we have presented an approach for constructing regional probabilistic climate change projections using a simple climate model, GCM simulations and skill scores. The approach is conceptually similar to other recent efforts [*Giorgi and Mearns*, 2003; *Tebaldi et al.*,

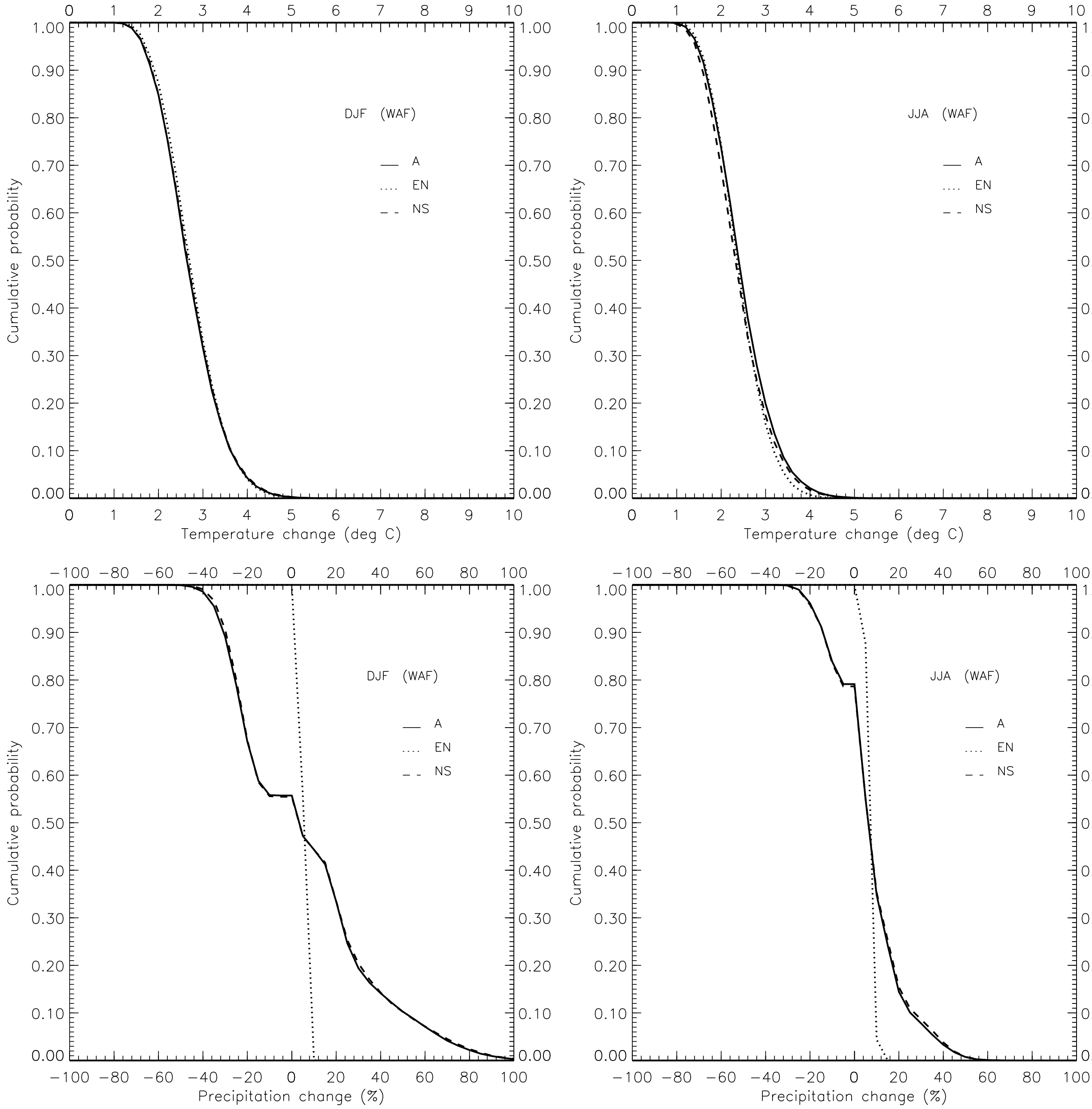


**Figure 5.** Regional cumulative probabilities of temperature and precipitation change for each season (DJF, JJA) for Western Africa under three different weighting schemes: using the combined skill score (A), using the ensemble mean (EN), and using no skill scores (NS). These probabilities are calculated for 2100 under the SRES A2 scenario family using the WR01 climate sensitivity PDF.

2004, 2005], but has the advantage of linking GCM regional projections to global temperature change projections from a simple climate model, which allows the quantification of further uncertainties through the pattern-scaling technique. Hence, the sensitivity of regional climate change projections to a range of uncertainty sources can be explored. This is important because even super ensembles (like the ones being developed at climateprediction.net) will have to use some sort of pattern-scaling to generate uncertainties for different emission scenarios, etc., because they could not run all combinations of plausible emission scenarios for each model version. An advantage of this approach to a perturbed physics approach that samples uncertainty in a single model is that we use the response patterns from several GCMs (a multi-model ensemble approach) that captures fundamental structural uncertainties between GCMs.

[30] The approach we have presented also has several limitations. The level of confidence in pattern-scaling technique, which is central to the methodology applied in the study, is not quantified, because of the absence of directly

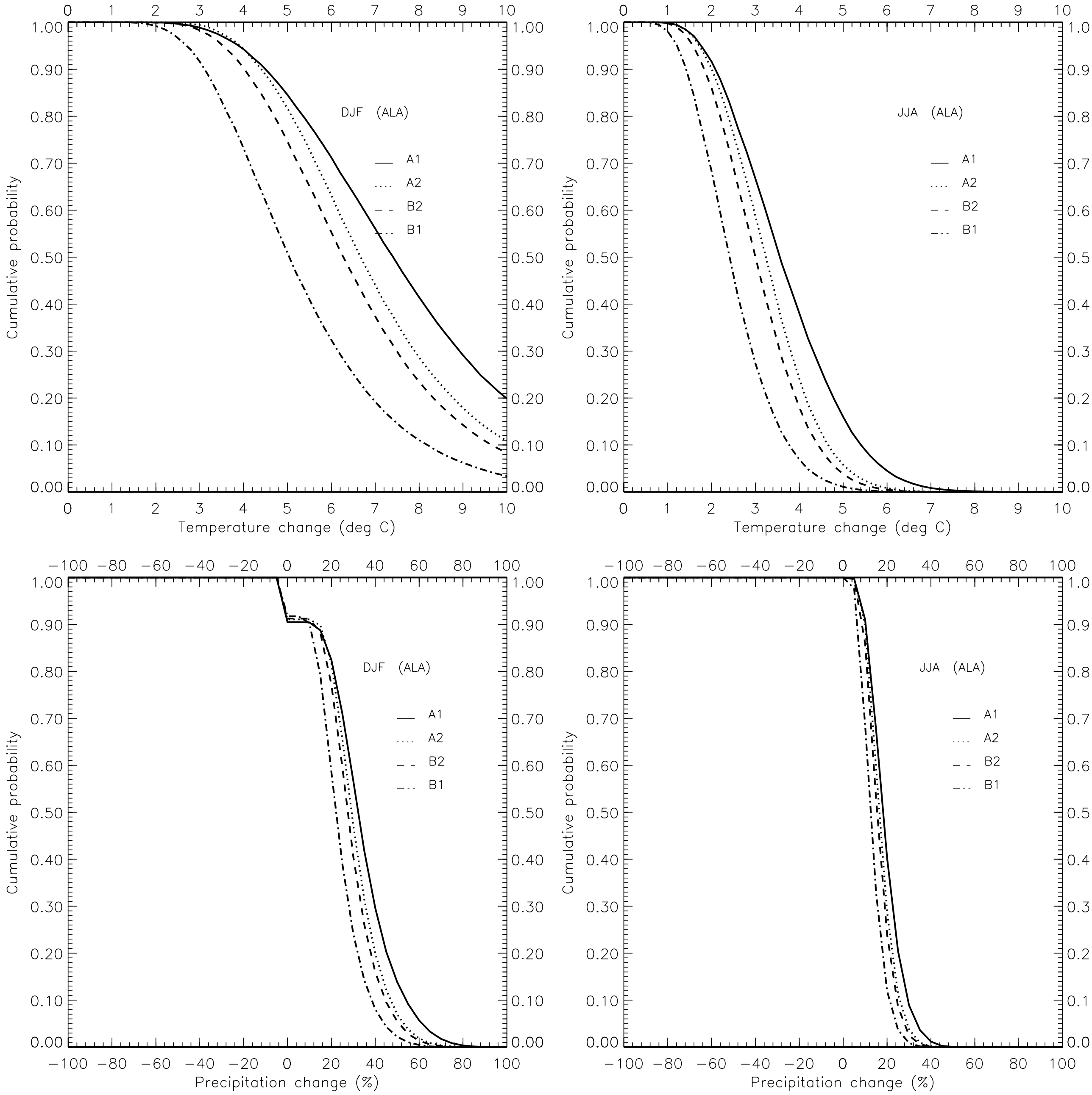


**Figure 6.** Regional cumulative probabilities of temperature and precipitation change for each season (DJF, JJA) for Alaska under the four SRES emissions scenario families: A1, A2, B2, and B1. These probabilities are calculated for 2100, using GCM weighting scheme A and the WR01 climate sensitivity PDF.

comparable GCM outputs to test the vigour of the technique. However, in a systematic exploration of patter-scaling, *Mitchell* [2003] concluded that at the grid box level the average error was only a small proportion of the average change. The regional skill scores also bring their own limitations because skill scores could be very different should different variables be chosen to measure model performance. ‘It has proved elusive to derive a fully comprehensive multidimensional “figure of merit” for climate models’ [*McAvaney et al.*, 2001]. We are not claiming comprehensiveness with our skill scores approach, but exploring some plausible approaches. The use of skill scores opens up a number of questions for climate research: At what scale should we measure skill (global, regional, grid box)? Should we focus on the variable of interest or a range of variables? How do we convert skill scores into probability? There is subjectivity in weighting the skill scores so perhaps eliciting expert opinions would be appropriate in the future. Another caveat of this approach is that it focuses exclusively on the anthropogenic signal at different time periods and ignores natural variability. For actual use in risk management these probabilities would have to

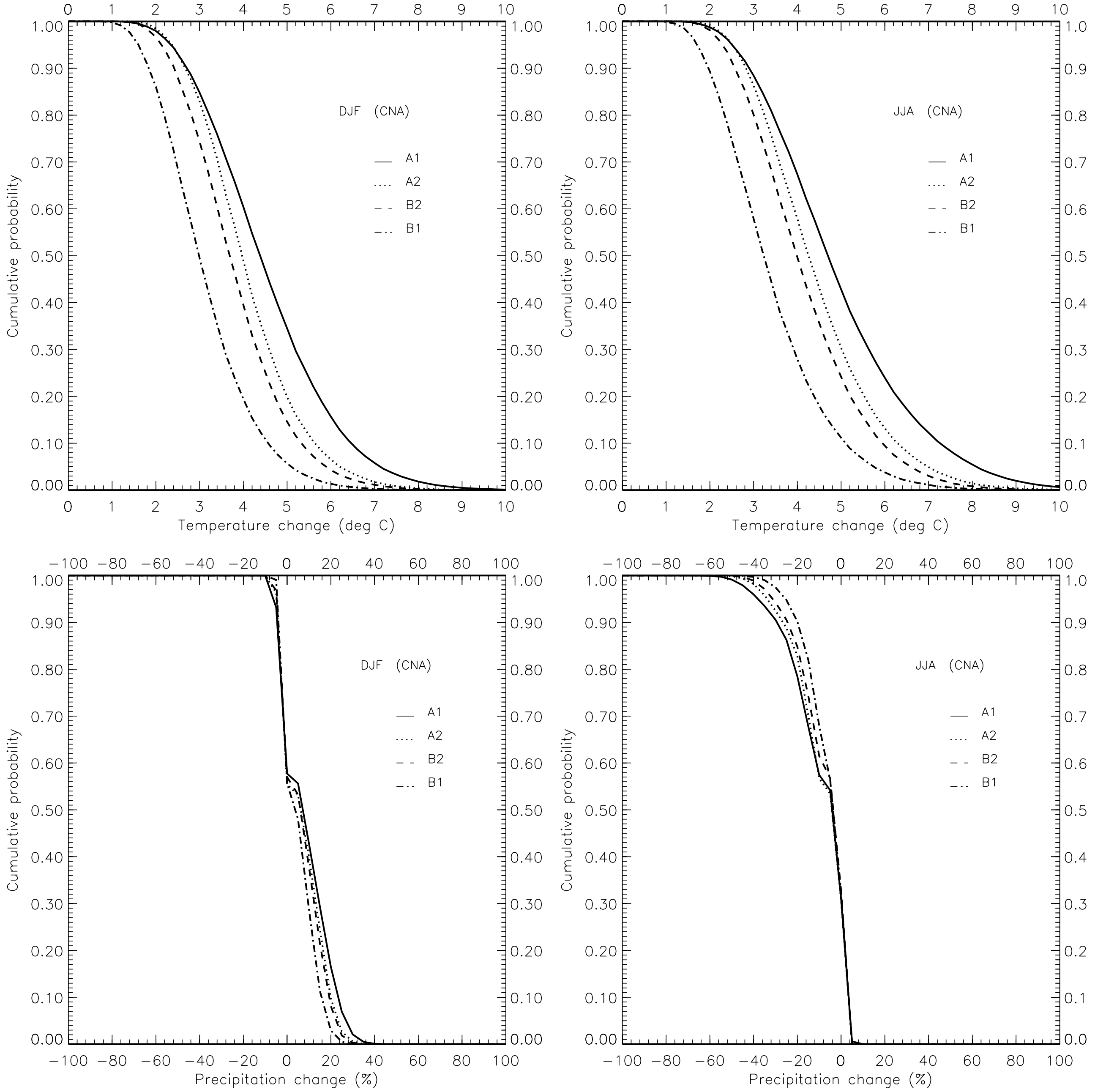


**Figure 7.** Regional cumulative probabilities of temperature and precipitation change for each season (DJF, JJA) for Central North America under the four SRES emissions scenario families: A1, A2, B2, and B1. These probabilities are calculated for 2100, using GCM weighting scheme A and the WR01 climate sensitivity PDF.

include natural multi-decadal climate variability [*Hulme et al.*, 1999].

[31] It was shown that using the skill scores did not make a substantial difference from not using them. However, either of these approaches provide more information than simply using the multi-model ensemble average, which corroborates the findings of *Murphy et al.* [2004] that scaling a single response pattern drastically underestimates the uncertainty in tropical precipitation. In general, regional temperature change was insensitive to GCM weighting scheme and most sensitive to emission scenario uncertainty followed by climate sensitivity. For precipitation change sensitivities are region specific, but all three tested uncertainties introduce large uncertainties to the projection (on average between 5–23% precipitation change).

[32] This framework provides a simple approach for the construction of regional projections of climate change that quantify uncertainties explicitly and consistently. Uncertainty quantification in regional climate change projections is particularly important if such projections are to be used in risk management approaches to adaptation. While we have not demonstrated the potential application

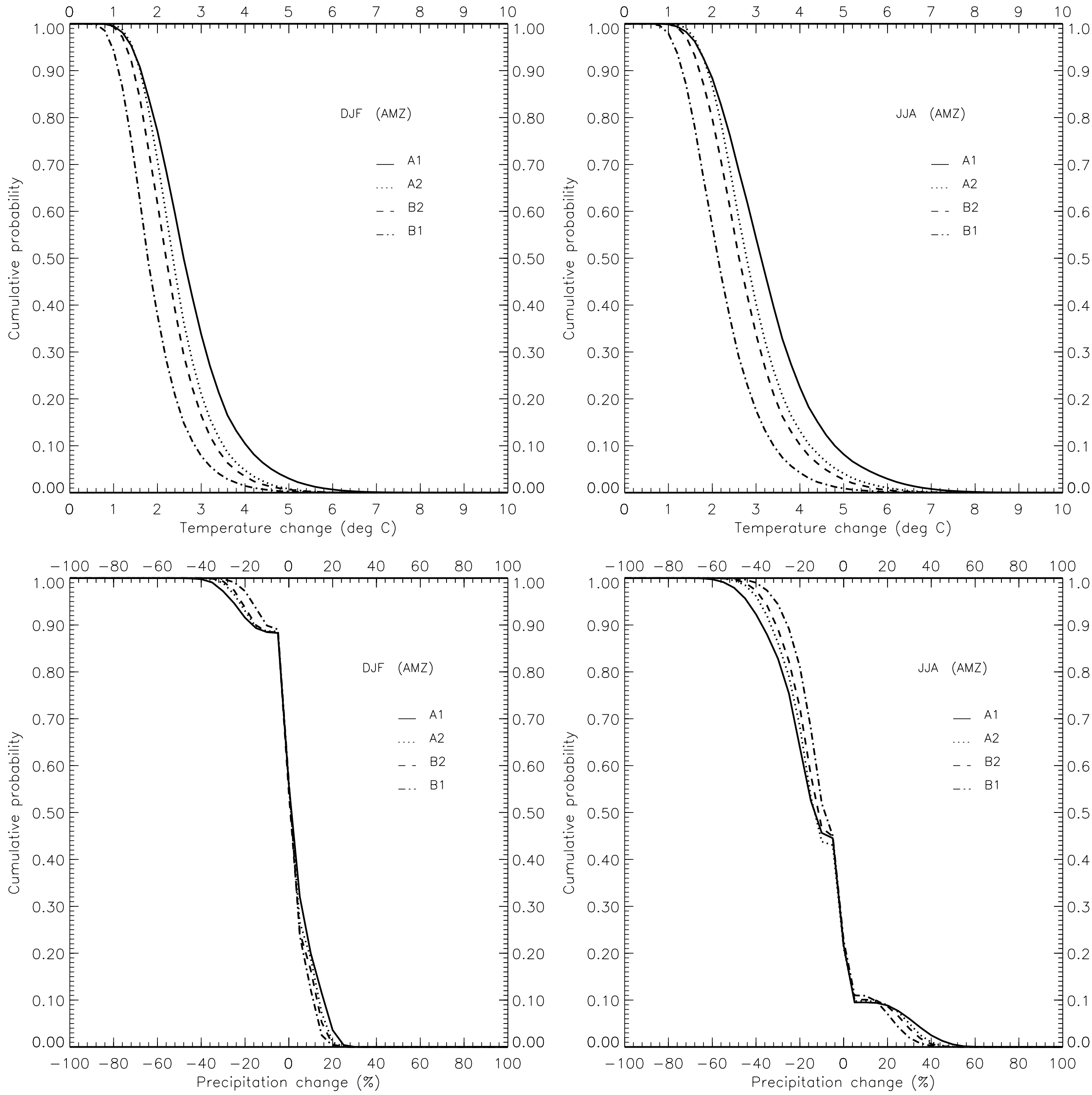


**Figure 8.** Regional cumulative probabilities of temperature and precipitation change for each season (DJF, JJA) for Amazonia under the four SRES emissions scenario families: A1, A2, B2, and B1. These probabilities are calculated for 2100, using GCM weighting scheme A and the WR01 climate sensitivity PDF.

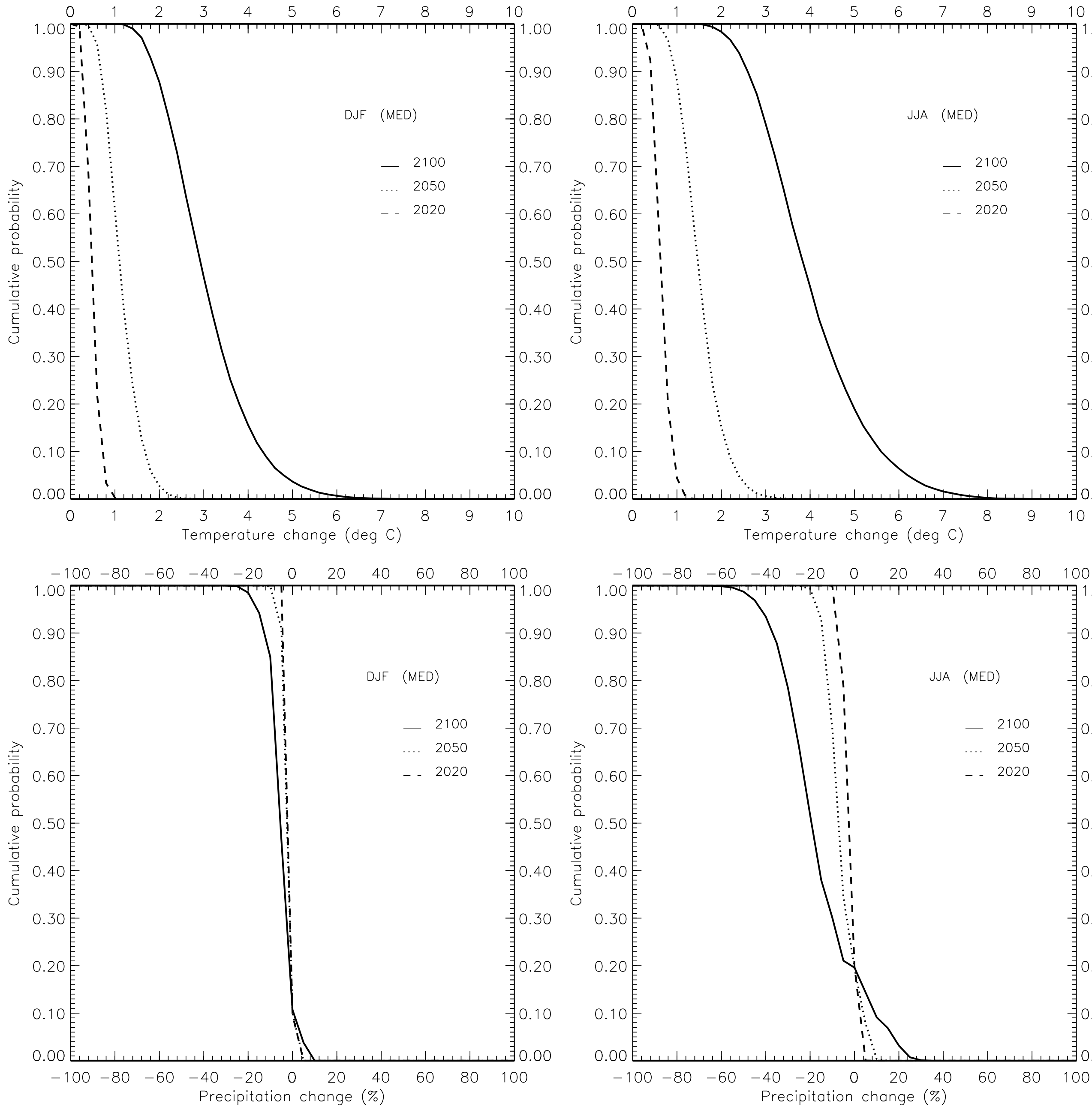


**Figure 9.** Regional cumulative probabilities of temperature and precipitation change for each season (DJF, JJA) for the Mediterranean for different time horizons: 2020, 2050, and 2100. These probabilities are calculated with weighting scheme A, under the SRES A2 family using the WR01 climate sensitivity PDF.

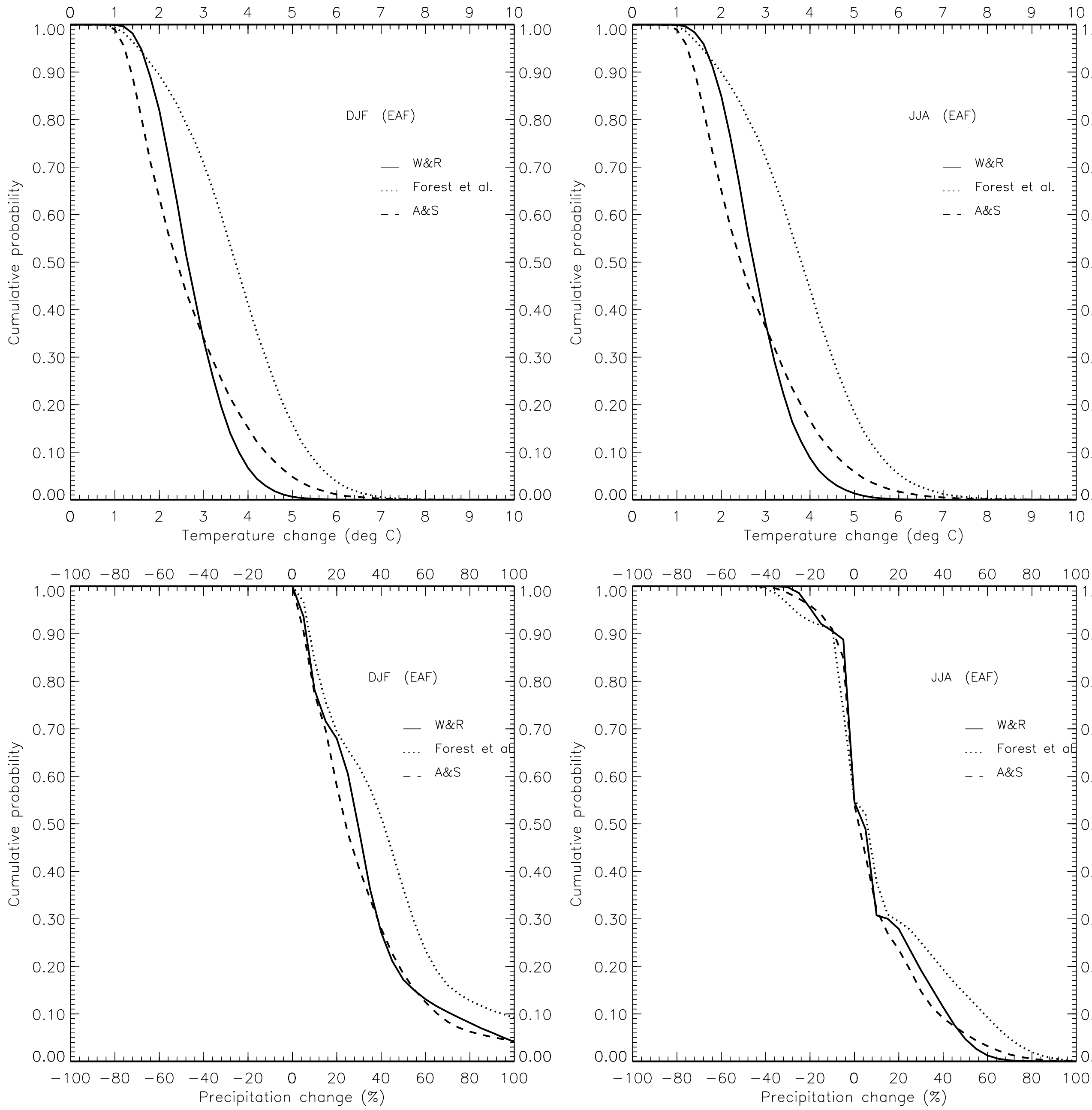


**Figure 10.** Regional cumulative probabilities of temperature and precipitation change for each season (DJF, JJA) for East Africa using different PDFs for climate sensitivity, namely: WR01, *Forest et al.* [2002], and *Andronova and Schlesinger* [2001]. These probabilities are calculated for 2100, with weighting scheme A under the SRES A2 family.

**Table 4.** Sensitivity Analysis of Regional Climate Change Probabilities to Uncertainties in GCM Weighting Schemes (GCMs), Climate Sensitivity (Sens.), and Greenhouse Gas Emissions (SRES)[a]

| | 95% | | | 50% | | | 5% | | |
|---|---|---|---|---|---|---|---|---|---|
| | | | | *Temperature* | | | | | |
| DJF | GCMs | Sens. | SRES | GCMs | Sens. | SRES | GCMs | Sens. | SRES |
| NAU | 0.16 | 0.42 | 2.09 | 0.10 | 0.98 | 1.51 | 0.33 | 1.69 | 1.38 |
| AMZ | 0.14 | 0.28 | 1.97 | 0.15 | 0.84 | 1.45 | 0.61 | 2.03 | 1.59 |
| SSA | 0.04 | 0.30 | 1.72 | 0.06 | 0.81 | 1.24 | 0.20 | 1.33 | 1.16 |
| CAM | 0.11 | 0.26 | 1.95 | 0.11 | 0.87 | 1.40 | 0.16 | 1.67 | 1.27 |
| WNA | 0.26 | 0.45 | 3.12 | 0.07 | 1.40 | 2.27 | 1.24 | 2.82 | 2.24 |
| CAN | 0.40 | 0.49 | 3.27 | 0.28 | 1.45 | 2.33 | 1.01 | 2.73 | 2.34 |
| ENA | 0.19 | 0.42 | 2.75 | 0.18 | 1.16 | 1.98 | 0.78 | 2.34 | 1.92 |
| ALA | 0.70 | 0.87 | 5.90 | 0.53 | 2.60 | 4.30 | 2.37 | 5.42 | 4.55 |
| GRL | 0.36 | 0.80 | 5.34 | 0.34 | 2.27 | 3.79 | 1.41 | 5.02 | 4.03 |
| MED | 0.27 | 0.37 | 2.45 | 0.27 | 1.11 | 1.86 | 0.72 | 2.45 | 1.83 |
| NEU | 0.90 | 0.47 | 4.22 | 0.92 | 1.38 | 3.23 | 2.94 | 4.66 | 4.17 |
| WAF | 0.08 | 0.32 | 2.12 | 0.08 | 0.96 | 1.51 | 0.10 | 1.75 | 1.38 |
| EAF | 0.14 | 0.34 | 2.17 | 0.08 | 0.81 | 1.55 | 0.35 | 1.72 | 1.55 |
| SAF | 0.03 | 0.30 | 1.77 | 0.04 | 0.77 | 1.23 | 0.26 | 1.34 | 1.13 |
| SAH | 0.16 | 0.43 | 2.85 | 0.12 | 1.35 | 2.03 | 0.51 | 2.87 | 1.95 |
| SEA | 0.02 | 0.28 | 1.64 | 0.01 | 0.79 | 1.16 | 0.08 | 1.34 | 1.05 |
| EAS | 0.17 | 0.44 | 2.87 | 0.21 | 1.46 | 2.02 | 0.75 | 3.19 | 1.77 |
| SAS | 0.05 | 0.44 | 2.29 | 0.03 | 1.14 | 1.66 | 0.23 | 1.86 | 1.49 |
| CAS | 0.39 | 0.45 | 3.22 | 0.26 | 1.42 | 2.34 | 0.70 | 2.82 | 2.40 |
| TIB | 0.32 | 0.57 | 3.75 | 0.28 | 1.69 | 2.63 | 0.39 | 3.21 | 2.47 |
| NAS | 0.45 | 0.98 | 5.18 | 0.41 | 2.55 | 3.76 | 1.46 | 4.88 | 3.80 |
| SAU | 0.19 | 0.24 | 1.68 | 0.14 | 0.75 | 1.20 | 0.23 | 1.32 | 1.11 |
| Average | 0.25 | 0.45 | 2.85 | 0.21 | 1.30 | 2.11 | 0.77 | 2.66 | 2.12 |
| | | | | *Precipitation* | | | | | |
| DJF | GCMs | Sens. | SRES | GCMs | Sens. | SRES | GCMs | Sens. | SRES |
| NAU | 14.19 | 4.86 | 17.01 | 4.50 | 0.27 | 6.17 | 17.96 | 9.76 | 8.99 |
| AMZ | 27.23 | 11.33 | 29.38 | 6.55 | 1.55 | 7.20 | 16.21 | 8.49 | 6.52 |
| SSA | 8.41 | 3.71 | 8.68 | 3.05 | 1.24 | 3.22 | 8.59 | 3.82 | 3.42 |
| CAM | 17.72 | 13.86 | 19.85 | 3.94 | 6.79 | 4.58 | 15.98 | 3.74 | 3.62 |
| WNA | 8.16 | 0.80 | 13.00 | 4.58 | 2.41 | 8.79 | 14.38 | 12.85 | 8.27 |
| CAN | 9.53 | 2.61 | 12.97 | 6.05 | 0.46 | 8.65 | 17.03 | 10.43 | 9.59 |
| ENA | 7.42 | 1.33 | 11.88 | 1.93 | 1.62 | 5.30 | 4.70 | 7.08 | 5.96 |
| ALA | 16.63 | 0.30 | 32.62 | 5.10 | 7.63 | 18.34 | 15.65 | 26.44 | 17.97 |
| GRL | 13.50 | 2.65 | 31.14 | 12.11 | 8.65 | 22.85 | 20.30 | 28.31 | 25.27 |
| MED | 10.60 | 8.38 | 11.58 | 3.65 | 4.13 | 3.14 | 8.52 | 2.44 | 2.03 |
| NEU | 6.05 | 1.28 | 15.85 | 6.14 | 4.08 | 12.26 | 13.04 | 16.16 | 15.19 |
| WAF | 41.08 | 17.70 | 47.02 | 27.76 | 19.28 | 25.07 | 71.59 | 32.42 | 32.45 |
| EAF | 15.65 | 1.51 | 36.32 | 16.97 | 10.20 | 27.28 | 64.52 | 49.76 | 43.37 |
| SAF | 12.16 | 4.90 | 10.86 | 5.53 | 1.10 | 5.13 | 7.41 | 3.33 | 2.95 |
| SAH | 76.14 | 0.00 | 83.36 | 33.84 | 16.66 | 40.33 | 69.01 | 35.29 | 22.21 |
| SEA | 6.75 | 2.08 | 8.29 | 3.40 | 1.82 | 4.16 | 9.80 | 5.75 | 4.31 |
| EAS | 11.69 | 2.65 | 17.60 | 6.82 | 0.44 | 12.36 | 22.42 | 16.66 | 14.70 |
| SAS | 29.95 | 13.50 | 31.09 | 4.62 | 4.98 | 5.15 | 18.77 | 6.66 | 5.92 |
| CAS | 16.95 | 4.05 | 23.67 | 7.63 | 2.71 | 11.83 | 29.21 | 20.31 | 17.10 |
| TIB | 54.51 | 15.87 | 67.50 | 21.66 | 15.32 | 30.56 | 21.10 | 19.39 | 14.25 |
| NAS | 12.69 | 2.83 | 35.20 | 3.87 | 9.62 | 21.67 | 17.63 | 24.80 | 24.84 |
| SAU | 17.28 | 7.27 | 16.82 | 6.86 | 3.18 | 7.01 | 28.34 | 10.91 | 11.24 |
| Average | 19.74 | 5.61 | 25.68 | 8.93 | 5.64 | 13.23 | 23.28 | 16.13 | 13.64 |

[a]The top part of the table is for temperature (degree C change), and the bottom part is for precipitation (% change), both for DJF.

**Table 5.** Probabilities of Exceeding Thresholds of Regional Temperature and Precipitation Change for 2100 Under SRES A2 Scenarios, WR01 Climate Sensitivity PDF, and GCM Weighting Scheme A[a]

| | Temperature | | | | | |
|---|---|---|---|---|---|---|
| | DJF | | | JJA | | |
| Region | >2K | >4K | >6K | >2K | >4K | >6K |
| SAU | 0.55 (0.88) | 0.00 (0.00) | 0.00 (0.00) | 0.53 (0.76) | 0.01 (0.00) | 0.00 (0.00) |
| AMZ | 0.70 (0.72) | 0.04 (0.15) | 0.00 (0.00) | 0.88 (0.87) | 0.12 (0.28) | 0.01 (0.03) |
| WNA | 0.98 (0.99) | 0.43 (0.35) | 0.06 (0.11) | 0.98 (0.99) | 0.32 (0.70) | 0.03 (0.24) |
| CAN | 0.99 (0.91) | 0.49 (0.49) | 0.06 (0.12) | 0.99 (0.99) | 0.61 (0.64) | 0.14 (0.13) |
| MED | 0.88 (0.96) | 0.14 (0.03) | 0.01 (0.01) | 0.98 (0.99) | 0.40 (0.24) | 0.05 (0.03) |
| NEU | 0.99 (0.90) | 0.61 (0.44) | 0.22 (0.06) | 0.93 (0.97) | 0.16 (0.40) | 0.00 (0.08) |
| WAF | 0.84 (0.94) | 0.04 (0.24) | 0.00 (0.00) | 0.75 (0.83) | 0.02 (0.09) | 0.00 (0.00) |
| SAF | 0.66 (0.95) | 0.01 (0.19) | 0.00 (0.00) | 0.74 (0.96) | 0.01 (0.22) | 0.00 (0.00) |
| EAS | 0.98 (1.00) | 0.30 (0.55) | 0.02 (0.23) | 0.91 (0.97) | 0.16 (0.34) | 0.01 (0.02) |
| SAS | 0.91 (0.98) | 0.09 (0.24) | 0.00 (0.01) | 0.62 (0.46) | 0.00 (0.00) | 0.00 (0.00) |
| | Precipitation | | | | | |
| | DJF | | | JJA | | |
| Region | <10% | >0% | >10% | <10% | >0% | >10% |
| SAU | 0.15 (0.11) | 0.39 (0.83) | 0.11 (0.42) | 0.30 (0.23) | 0.10 (0.18) | 0.00 (0.00) |
| AMZ | 0.10 (0.02) | 0.62 (0.91) | 0.16 (0.02) | 0.62 (0.03) | 0.18 (0.10) | 0.08 (0.02) |
| WNA | 0.00 (0.00) | 0.92 (0.85) | 0.54 (0.09) | 0.42 (0.01) | 0.29 (0.32) | 0.01 (0.01) |
| CAN | 0.00 (0.09) | 0.62 (0.41) | 0.43 (0.06) | 0.37 (0.57) | 0.26 (0.24) | 0.00 (0.00) |
| MED | 0.13 (0.06) | 0.09 (0.31) | 0.00 (0.00) | 0.60 (0.80) | 0.31 (0.13) | 0.08 (0.05) |
| NEU | 0.00 (0.00) | 1.00 (1.00) | 0.76 (0.71) | 0.00 (0.19) | 0.77 (0.37) | 0.13 (0.00) |
| WAF | 0.38 (0.03) | 0.62 (0.93) | 0.52 (0.50) | 0.14 (0.04) | 0.82 (0.56) | 0.44 (0.00) |
| SAF | 0.03 (0.00) | 0.70 (0.53) | 0.00 (0.13) | 0.80 (0.70) | 0.00 (0.18) | 0.00 (0.00) |
| EAS | 0.00 (0.04) | 0.73 (0.82) | 0.58 (0.50) | 0.00 (0.00) | 1.00 (1.00) | 0.53 (0.33) |
| SAS | 0.08 (0.38) | 0.47 (0.25) | 0.07 (0.06) | 0.00 (0.00) | 0.91 (1.00) | 0.86 (0.81) |

[a]Numbers in parentheses are those from *Giorgi and Mearns* [2003].

of regional climate change probabilities this has been done by several authors in several different contexts. For example, *New and Hulme* [2000] propagated regional climate change probabilities into a catchment hydrological model to examine river flow changes. Similarly, *Jones* [2000a] used regional climate change probabilities with an irrigation demand model to analyse the probability of exceeding a critical threshold where adaptation was required. There are various other hypothetical [*Räisänen and Palmer*, 2001] and applied [*Prudhomme et al.*, 2003] examples of applying regional climate change probabilities to real world problems. What this paper shows is that there is a range of uncertainties that adaptation decisions need to be tested against if they are to be deemed robust. Of course, this is a limited sensitivity analysis based on data that is currently publicly available and does not address downscaling issues. In the future, when large number (e.g., thousands) of GCM simulations become available, such frameworks will become increasingly more relevant and hopefully more robust.

[33] **Acknowledgments.** Suraje Dessai is supported by a grant (SFRH/BD/4901/2001) from Fundação para a Ciência e a Tecnologia, in Portugal. The Tyndall Centre for Climate Change Research is core funded by three UK research councils, NERC, EPSRC, and ESRC, and receives additional support from the UK Department of Trade and Industry. Tom Wigley and Sarah Raper are thanked for the use of their model. Authors of the climate sensitivity studies are thanked for the data provided. The original GCM simulation outputs were interpolated onto a 2.5 by 2.5 degree grid by Richard Jones at the Hadley Centre. We are grateful to three anonymous reviewers for their useful comments.

## References

Adger, W. N., N. W. Arnell, and E. L. Tompkins (2005), Successful adaptation to climate change across scales, *Global Environ. Change*, *15*(2), 77–86.

Allen, M. (2001), Do-it-yourself climate prediction, *Nature*, *401*(6754), 642.

Andronova, N. G., and M. E. Schlesinger (2001), Objective estimation of the probability density function for climate sensitivity, *J. Geophys. Res.*, *106*(D19), 22,605–22,611.

Benestad, R. E. (2004), Tentative probabilistic temperature scenarios for northern Europe, *Tellus, Ser. A*, *56*(2), 89–101.

Boville, B. A., J. T. Kiehl, P. J. Rasch, and F. O. Bryan (2001), Improvements to the NCAR CSM-1 for transient climate simulations, *J. Clim.*, *14*(2), 164–179.

Carter, T. R., E. L. La Rovere, R. N. Jones, R. Leemas, L. O. Mearns, N. Nakicenovic, A. B. Pittock, S. M. Semenov, and J. Skea (2001), Developing and applying scenarios, in *Climate Change 2001: Impacts, Adaptation, and Vulnerability*, edited by Intergovernmental Panel on Climate Change, pp. 145–190, Cambridge Univ. Press, New York.

Dessai, S., and M. Hulme (2001), Climatic implications of revised IPCC emission scenarios, the Kyoto Protocol and quantification of uncertainties, *Integrated Assess.*, *2*(3), 159–170.

Dixon, K. W., and J. R. Lanzante (1999), Global mean surface air temperature and North Atlantic overturning in a suite of coupled GCM climate change experiments, *Geophys. Res. Lett.*, *26*(13), 1885–1888.

Ekström, M., B. Hingray, A. Mezghani, and P. D. Jones (2005), Regional climate model data used within the SWURVE project 2: Addressing uncertainty in regional climate model data for five European case study areas, *Hydrol. Earth Syst. Sci.*, in press.

Flato, G. M., and G. J. Boer (2001), Warming asymmetry in climate change simulations, *Geophys. Res. Lett.*, *28*(1), 195–198.

Forest, C. E., P. H. Stone, A. P. Sokolov, M. R. Allen, and M. D. Webster (2002), Quantifying uncertainties in climate system properties with the use of recent climate observations, *Science*, *295*(5552), 113–117.

Gates, W. L., A. Henderson-Sellers, G. J. Boer, C. K. Folland, A. Kitoh, B. J. McAvaney, F. Semazzi, N. Smith, A. J. Weaver, and Q.-C. Zeng (1996), Climate models - Evaluation, in *Climate Change 1995: The Science of Climate Change*, edited by J. T. Houghton et al., pp. 229–284, Cambridge Univ. Press, New York.

Gates, W. L., et al. (1999), An overview of the results of the Atmospheric Model Intercomparison Project (AMIP I), *Bull. Am. Meteorol. Soc.*, *80*(1), 29–55.

Giorgi, F., and R. Francisco (2000a), Evaluating uncertainties in the prediction of regional climate change, *Geophys. Res. Lett.*, *27*(9), 1295–1298.

Giorgi, F., and R. Francisco (2000b), Uncertainties in regional climate change prediction: A regional analysis of ensemble simulations with the HADCM2 coupled AOGCM, *Clim. Dyn.*, *16*(2–3), 169–182.

Giorgi, F., and L. O. Mearns (2002), Calculation of average, uncertainty range, and reliability of regional climate changes from AOGCM simula-

tions via the "reliability ensemble averaging" (REA) method, *J. Clim.*, *15*(10), 1141–1158.
Giorgi, F., and L. O. Mearns (2003), Probability of regional climate change based on the Reliability Ensemble Averaging (REA) method, *Geophys. Res. Lett.*, *30*(12), 1629, doi:10.1029/2003GL017130.
Gordon, C., C. Cooper, C. A. Senior, H. Banks, J. M. Gregory, T. C. Johns, J. F. B. Mitchell, and R. A. Wood (2000), The simulation of SST, sea ice extents and ocean heat transports in a version of the Hadley Centre coupled model without flux adjustments, *Clim. Dyn.*, *16*(2–3), 147–168.
Gordon, H. B., and S. P. O'Farrell (1997), Transient climate change in the CSIRO coupled model with dynamic sea ice, *Mon. Weather Rev.*, *125*(5), 875–907.
Gregory, J. M., R. J. Stouffer, S. C. B. Raper, P. A. Stott, and N. A. Rayner (2002), An observationally based estimate of the climate sensitivity, *J. Clim.*, *15*(22), 3117–3121.
Houghton, J. T., Y. Ding, D. J. Griggs, M. Noguer, P. J. van der Linden, X. Dai, K. Maskell, and C. A. Johnson (2001), *Climate Change 2001: The Scientific Basis*, Cambridge Univ. Press, New York.
Hulme, M., and O. Brown (1998), Portraying climate scenario uncertainties in relation to tolerable regional climate change, *Clim. Res.*, *10*(1), 1–14.
Hulme, M., E. M. Barrow, N. W. Arnell, P. A. Harrison, T. C. Johns, and T. E. Downing (1999), Relative impacts of human-induced climate change and natural climate variability, *Nature*, *397*(6721), 688–691.
Jones, R. N. (2000a), Analysing the risk of climate change using an irrigation demand model, *Clim. Res.*, *14*(2), 89–100.
Jones, R. N. (2000b), Managing uncertainty in climate change projections - Issues for impact assessment, *Clim. Change*, *45*(3–4), 403–419.
Kittel, T. G. F., F. Giorgi, and G. A. Meehl (1998), Intercomparison of regional biases and doubled $CO_2$-sensitivity of coupled atmosphere-ocean general circulation model experiments, *Clim. Dyn.*, *14*, 1–15.
Knutti, R., T. F. Stocker, F. Joos, and G. K. Plattner (2002), Constraints on radiative forcing and future climate change from observations and climate model ensembles, *Nature*, *416*(6882), 719–723.
Lambert, S. J., and G. J. Boer (2001), CMIP1 evaluation and intercomparison of coupled climate models, *Clim. Dyn.*, *17*(2–3), 83–106.
MacCracken, M. C., E. Barron, D. Easterling, B. Felzer, and T. Karl (2001), Scenarios for climate variability and change, in *Climate Change Impacts on the United States*, edited by N. A. S. Team, pp. 13–71, Cambridge Univ. Press, New York.
McAvaney, B. J., C. Covey, S. Joussaume, V. Kattsov, A. Kitoh, W. Ogana, A. J. Pitman, A. J. Weaver, R. A. Wood, and Z.-C. Zhao (2001), Model evaluation, in *Climate Change 2001: The Scientific Basis*, edited by J. T. Houghton et al., pp. 471–523, Cambridge Univ. Press, New York.
Miranda, P., F. E. S. Coelho, A. R. Tomé, and M. A. Valente (2002), 20th century Portuguese climate and climate scenarios, in *Climate Change in Portugal. Scenarios, Impacts and Adaptation Measures - SIAM Project*, edited by F. D. Santos, K. Forbes, and R. Moita, pp. 23–83, Gradiva, Lisbon.
Mitchell, T. D. (2003), Pattern scaling - An examination of the accuracy of the technique for describing future climates, *Clim. Change*, *60*(3), 217–242.
Morgan, M. G., and D. W. Keith (1995), Climate-change - Subjective judgments by climate experts, *Environ. Sci. Technol.*, *29*(10), A468–A476.
Murphy, A. H. (1988), Skill scores based on the mean-square error and their relationships to the correlation-coefficient, *Mon. Weather Rev.*, *116*(12), 2417–2425.
Murphy, J. M., D. M. H. Sexton, D. N. Barnett, G. S. Jones, M. J. Webb, M. Collins, and D. A. Stainforth (2004), Quantifying uncertainties in climate change from a large ensemble of general circulation model predictions, *Nature*, *430*, 768–772.
Nakicenovic, N., et al. (2000), *Emissions Scenarios. A Special Report of Working Group III of the Intergovernmental Panel on Climate Change*, 599 pp., Cambridge Univ. Press, New York.
New, M., and M. Hulme (2000), Representing uncertainty in climate change scenarios: A Monte-Carlo approach, *Integrated Assess.*, *1*, 203–213.
New, M., M. Hulme, and P. Jones (1999), Representing twentieth-century space-time climate variability. part I: Development of a 1961–90 mean monthly terrestrial climatology, *J. Clim.*, *12*(3), 829–856.
Nozawa, T., S. Emori, T. Takemura, T. Nakajima, A. Numaguti, A. Abe-Ouchi, and M. Kimoto (2000), Coupled ocean-atmosphere model experiments of future climate change based on IPCC SRES scenarios, paper presented at 11th Symposium on Global Change Studies, Long Beach, Calif.
Palmer, T. N., and J. Räisänen (2002), Quantifying the risk of extreme seasonal precipitation events in a changing climate, *Nature*, *415*(6871), 512–514.
Parry, M., N. Arnell, M. Hulme, R. Nicholls, and M. Livermore (1998), Adapting to the inevitable, *Nature*, *395*(6704), 741.
Patwardhan, A., and M. J. Small (1992), Bayesian methods for model uncertainty analysis with application to future sea-level rise, *Risk Anal.*, *12*(4), 513–523.
Prudhomme, C., D. Jakob, and C. Svensson (2003), Uncertainty and climate change impact on the flood regime of small UK catchments, *J. Hydrol.*, *277*(1–2), 1–23.
Räisänen, J., and H. Alexandersson (2003), A probabilistic view on recent and near future climate change in Sweden, *Tellus, Ser. A*, *55*(2), 113–125.
Räisänen, J., and T. N. Palmer (2001), A probability and decision-model analysis of a multimodel ensemble of climate change simulations, *J. Clim.*, *14*(15), 3212–3226.
Roeckner, E., J. M. Oberhuber, A. Bacher, M. Christoph, and I. Kirchner (1996), ENSO variability and atmospheric response in a global coupled atmosphere-ocean GCM, *Clim. Dyn.*, *12*(11), 737–754.
Ruosteenoja, K., T. R. Carter, K. Jylhä, and H. Tuomenvirta (2003), Future climate in world regions: An intercomparison of model-based projections for the new IPCC emissions scenarios, Finn. Environ. Inst., Helsinki.
Santer, B. D., T. M. L. Wigley, M. E. Schlesinger, and J. F. B. Mitchell (1990), Developing climate scenarios from equilibrium GCM results, Max-Planck-Inst. für Meteorol., Hamburg, Germany.
Stainforth, D., J. Kettleborough, M. Allen, M. Collins, A. Heaps, and J. Murphy (2002), Distributed computing for public-interest climate modeling research, *Comput. Sci. Eng.*, *4*(3), 82–89.
Stainforth, D. A., et al. (2005), Uncertainty in predictions of the climate response to rising levels of greenhouse gases, *Nature*, *433*(7024), 403–406.
Stocker, T. F., et al. (2001), Physical climate processes and feedbacks, in *Climate Change 2001: The Scientific Basis*, edited by J. T. Houghton et al., Cambridge Univ. Press, New York.
Stott, P. A., and J. A. Kettleborough (2002), Origins and estimates of uncertainty in predictions of twenty-first century temperature rise, *Nature*, *416*(6882), 723–726.
Taylor, K. E. (2001), Summarizing multiple aspects of model performance in a single diagram, *J. Geophys. Res.*, *106*(D7), 7183–7192.
Tebaldi, C., L. O. Mearns, D. Nychka, and R. L. Smith (2004), Regional probabilities of precipitation change: A Bayesian analysis of multimodel simulations, *Geophys. Res. Lett.*, *31*, L24213, doi:10.1029/2004GL021276.
Tebaldi, C., R. L. Smith, D. Nychka, and L. O. Mearns (2005), Quantifying uncertainty in projections of regional climate change: A Bayesian approach to the analysis of multi-model ensembles, *J. Clim.*, *18*(10), 1524–1540.
Titus, J. G., and V. Narayanan (1996), The risk of sea level rise, *Clim. Change*, *33*(2), 151–212.
Tol, R. S. J., and A. F. de Vos (1998), A Bayesian statistical analysis of the enhanced greenhouse effect, *Clim. Change*, *38*(1), 87–112.
Visser, H., R. J. M. Folkert, J. Hoekstra, and J. J. De Wolff (2000), Identifying key sources of uncertainty in climate change projections, *Clim. Change*, *45*(3–4), 421–457.
Washington, W. M., et al. (2000), Parallel climate model (PCM) control and transient simulations, *Clim. Dyn.*, *16*(10–11), 755–774.
Watterson, I. G. (1996), Non-dimensional measures of climate model performance, *Int. J. Climatol.*, *16*(4), 379–391.
Webster, M., et al. (2003), Uncertainty analysis of climate change and policy response, *Clim. Change*, *61*(3), 295–320.
Wigley, T. M. L. (1999), The science of climate change: Global and U.S. perspectives, 51 pp., Pew Cent. on Global Clim. Change, Arlington, Va.
Wigley, T. M. L., and S. C. B. Raper (2001), Interpretation of high projections for global-mean warming, *Science*, *293*(5529), 451–454.
Yukimoto, S., M. Endoh, Y. Kitamura, A. Kitoh, T. Motoi, and A. Noda (2000), ENSO-like interdecadal variability in the Pacific Ocean as simulated in a coupled general circulation model, *J. Geophys. Res.*, *105*(C6), 13,945–13,963.

S. Dessai, M. Hulme, and X. Lu, School of Environmental Sciences, University of East Anglia, Norwich NR4 7TJ, UK. (s.dessai@uea.ac.uk)